

# Liquid-gas phase transition in hot asymmetric nuclear matter with density-dependent relativistic mean-field models

Guang-Hua Zhang<sup>1</sup> and Wei-Zhou Jiang<sup>1,2</sup>

<sup>1</sup> *Department of Physics, Southeast University, Nanjing 211189, China*

<sup>2</sup> *National Laboratory of Heavy Ion Accelerator, Lanzhou 730000, China*

---

## Abstract

The liquid-gas phase transition in hot asymmetric nuclear matter is studied within density-dependent relativistic mean-field models where the density dependence is introduced according to the Brown-Rho scaling and constrained by available data at low densities and empirical properties of nuclear matter. The critical temperature of the liquid-gas phase transition is obtained to be 15.7 MeV in symmetric nuclear matter falling on the lower edge of the small experimental error bars. In hot asymmetric matter, the boundary of the phase-coexistence region is found to be sensitive to the density dependence of the symmetry energy. The critical pressure and the area of phase-coexistence region increases clearly with the softening of the symmetry energy. The critical temperature of hot asymmetric matter separating the single-phase region from the two-phase region is analyzed to have a moderate sensitivity to the symmetry energy and is higher for the model possessing the softer symmetry energy.

*Key words:* Liquid-gas transition, relativistic mean-field models, symmetry energy

*PACS:* 21.65.Ef, 21.65.Cd, 64.10.+h

---

## 1 Introduction

The determination of the properties of hadronic matter at finite temperature and density is a fundamental problem in nuclear physics. At low densities, the so-called liquid-gas (LG) phase transition in nuclear matter may occur at sufficiently low temperatures

due to the van der Waals behavior of the nucleon-nucleon interaction. The study of the LG phase transition in intermediate energy heavy-ion collisions is of considerable interest over the last three decades. In the past, properties of the nuclear LG phase transition have been explored both experimentally and theoretically in a variety of works [1,2,3,4,5,6,7,8,9,10,11,12,13,14,15,16,17]. The calculated critical temperature of symmetric nuclear matter lies in a wide range, e.g., 13-24 MeV, for various phenomenological models [8,9,10,11,12,13].

To understand better the features of the LG phase transition in hot asymmetric nuclear matter, it is imperative to employ the nuclear equation of state (EOS) of asymmetric matter. Recent progress in experiments with radioactive beams provides us a great opportunity to constrain the nuclear EOS of asymmetric matter. However, the nuclear EOS of asymmetric matter, especially the density dependence of the symmetry energy, is still rather poorly known [17,18,19]. The study of the LG phase transition may open a possible window to constrain the nuclear EOS of asymmetric matter. In the past, the sensitivity of the LG phase transition to the density dependence of the symmetry energy was explored with the non-relativistic models in Ref. [15]. Similar work with the nonlinear relativistic mean-field (RMF) models can be found in Ref. [16]. In this work, we study the thermodynamic properties of the LG phase transition in hot asymmetric nuclear matter with density-dependent RMF models.

The density-dependent RMF models adopted in present work [20,21] feature the chiral limits at high densities with the in-medium hadron properties according to the Brown-Rho (BR) scaling [22,23]. These models achieved satisfactory success in describing the nuclear EOS of asymmetric matter, the large mass neutron stars, and ground-state properties of finite nuclei [20,21]. It was known that the associated parameters that describe the in-medium hadron properties are in agreement with those from microscopic calculations [24] or those extracted from recent experimental data at low densities [25,26,27]. In addition, the BR scaled NN interaction was succeeded in yielding the observed  $^{14}\text{C}$  beta decay suppression [28]. Therefore, it is appealing to adopt the models with the BR scaling to study the properties of the LG phase transition that occurs in the low-density region. The emphasis is put on the influence of the asymmetric nuclear EOS, especially the density dependence of the nuclear symmetry energy, on the properties of the LG phase transition.

## 2 Formalism

The Lagrangian density of the density-dependent RMF models is written as

$$\begin{aligned}
\mathcal{L} = & \bar{\psi} \left[ i\gamma_\mu \partial^\mu - M^* + g_\sigma^* \sigma - g_\omega^* \gamma_\mu \omega^\mu - g_\rho^* \gamma_\mu \tau_3 b_0^\mu \right] \psi \\
& + \frac{1}{2} \left( \partial_\mu \sigma \partial^\mu \sigma - m_\sigma^{*2} \sigma^2 \right) - \frac{1}{4} F_{\mu\nu} F^{\mu\nu} + \frac{1}{2} m_\omega^{*2} \omega_\mu \omega^\mu \\
& - \frac{1}{4} B_{\mu\nu} B^{\mu\nu} + \frac{1}{2} m_\rho^{*2} b_{0\mu} b_0^\mu,
\end{aligned} \tag{1}$$

where  $\psi, \sigma, \omega$ , and  $b_0$  are the fields of the nucleon, scalar, vector, and isovector-vector mesons, with their in-medium scaled masses  $M^*, m_\sigma^*, m_\omega^*$ , and  $m_\rho^*$ , respectively.  $F_{\mu\nu}, B_{\mu\nu}$  are the strength tensors of  $\omega$  and  $\rho$  mesons, respectively

$$F_{\mu\nu} = \partial_\mu \omega_\nu - \partial_\nu \omega_\mu, \quad B_{\mu\nu} = \partial_\mu b_{0\nu} - \partial_\nu b_{0\mu}, \tag{2}$$

$g_\sigma^*, g_\omega^*$ , and  $g_\rho^*$  are the coupling constants of the scalar, vector and isovector-vector mesons with nucleons, respectively. The meson coupling constants and hadron masses with asterisks denote the density dependence, given by the BR scaling [20,21,22].

In the mean-field approximation, the energy density and pressure at the finite temperature are given as

$$\begin{aligned}
\varepsilon = & \frac{1}{2} C_\omega^2 \rho_B^2 + \frac{1}{2} C_\rho^2 \rho_B^2 \alpha^2 + \frac{1}{2} \tilde{C}_\sigma^2 (m_N^* - M^*)^2 \\
& + \sum_{\tau=p,n} \frac{2}{(2\pi)^3} \int d^3 k E^* [n_\tau(k) + \bar{n}_\tau(k)],
\end{aligned} \tag{3}$$

and

$$\begin{aligned}
p = & \frac{1}{2} C_\omega^2 \rho_B^2 + \frac{1}{2} C_\rho^2 \rho_B^2 \alpha^2 - \frac{1}{2} \tilde{C}_\sigma^2 (m_N^* - M^*)^2 - \Sigma_0 \rho_B \\
& + \frac{1}{3} \sum_{\tau=p,n} \frac{2}{(2\pi)^3} \int d^3 k \frac{\mathbf{k}^2}{E^*} [n_\tau(k) + \bar{n}_\tau(k)],
\end{aligned} \tag{4}$$

where  $C_\omega = g_\omega^*/m_\omega^*$ ,  $C_\rho = g_\rho^*/m_\rho^*$ ,  $\tilde{C}_\sigma = m_\sigma^*/g_\sigma^*$ ,  $E^* = \sqrt{\vec{k}^2 + m_N^{*2}}$  with  $m_N^* = M^* - g_\sigma^* \sigma$  the effective mass of nucleon,  $\alpha$  is the isospin asymmetry parameter being  $\alpha = (\rho_n - \rho_p)/\rho_B$  with  $\rho_B = \rho_n + \rho_p$ , and  $\Sigma_0$  is the rearrangement term originating from the density dependence of the parameters,

$$\begin{aligned}
\Sigma_0 = & -\rho_B^2 C_\omega \frac{\partial C_\omega}{\partial \rho_B} - \rho_B^2 \alpha^2 C_\rho \frac{\partial C_\rho}{\partial \rho_B} \\
& - \tilde{C}_\sigma \frac{\partial \tilde{C}_\sigma}{\partial \rho_B} (m_N^* - M^*)^2 - \rho_s \frac{\partial M^*}{\partial \rho_B}.
\end{aligned} \tag{5}$$

The distribution functions  $n_\tau(k)$  and  $\bar{n}_\tau(k)$  for nucleon and antinucleon are given as

$$n_\tau(k) = \{\exp[(E^*(k) - \nu_\tau)/k_B T] + 1\}^{-1},$$

$$\bar{n}_\tau(k) = \{\exp[(E^*(k) + \nu_\tau)/k_B T] + 1\}^{-1} \quad (\tau = n, p),$$

where the effective chemical potentials for nucleons read

$$\nu_\tau = \mu_\tau - g_\omega^* \omega \pm g_\rho^* b_0 + \Sigma_0, \quad (6)$$

with  $+$  in  $\pm$  for neutrons and  $-$  for protons. The chemical potentials or effective chemical potentials for nucleons can be determined from the nucleon densities

$$\rho_\tau = \frac{2}{(2\pi)^3} \int d^3k [n_\tau(k) - \bar{n}_\tau(k)]. \quad (7)$$

With the density-dependent RMF models, we can now study the LG phase transition. In this study, we do not consider the finite size effect and thus assume as usual the matter is homogeneous. The two phase coexistence is governed by the Gibb's conditions:

$$\mu_\tau(T, \rho_\tau^L) = \mu_\tau(T, \rho_\tau^G), \quad (8)$$

$$p(T, \rho_\tau^L) = p(T, \rho_\tau^G), \quad (9)$$

where L and G stand for the liquid and gas phase, respectively. The Gibbs conditions (8) and (9) require the same pressures and chemical potentials for two phases at different densities and isospin asymmetries. The stability conditions are given by

$$\rho_B \left( \frac{\partial p}{\partial \rho_B} \right)_{T, \alpha} > 0, \quad (10)$$

$$\left( \frac{\partial \mu_p}{\partial \alpha} \right)_{T, p} < 0, \text{ or } \left( \frac{\partial \mu_n}{\partial \alpha} \right)_{T, p} > 0. \quad (11)$$

### 3 Results and discussion

We first discuss the liquid-gas phase transition in symmetric nuclear matter with the density-dependent RMF models SLC and SLCd that only differ in the density dependence of the symmetry energy [21]. In Fig. 1, we show the pressure of symmetric matter as a function of nucleon density at various temperatures. At the low temperature, the pressure first increases and then decreases with the increasing density. The  $p$ - $\rho_B$  isotherms exhibit the form of the two phase coexistence, with a mechanically unstable region for each. In both models that share the same EOS of symmetric matter [21], there appears an equal critical point at temperature  $T = 15.7$  MeV, where  $\partial p / \partial \rho_B = 0$ , and  $\partial^2 p / \partial^2 \rho_B = 0$ . This temperature is called the critical temperature beyond which

symmetric nuclear matter can only be in a single phase. The experimental value of the critical temperature extracted for symmetric matter is  $16.6 \pm 0.9$  MeV [10], while our prediction is situated on the lower error bar.

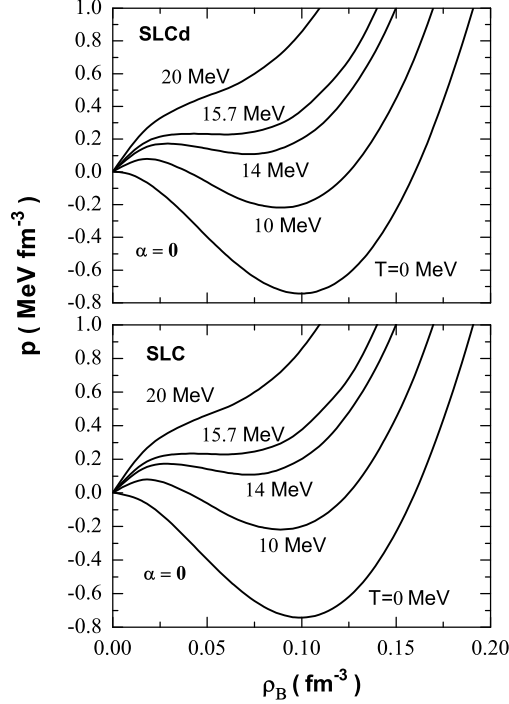


Fig. 1. The pressure of symmetric nuclear matter versus the nucleon density  $\rho_B$  at different temperatures in models SLCd and SLC.

In symmetric matter, the LG phase transition should be of first order, whereas in asymmetric matter it was recognized to be of second order [5,14]. In hot asymmetric matter, we can nevertheless obtain a temperature, denoted as  $T_{asy}$ , at a fixed  $\alpha$  similarly according to the relation  $\partial p / \partial \rho_B = \partial^2 p / \partial^2 \rho_B = 0$ . We show in Fig. 2 the  $T_{asy}$  as a function of  $\alpha$  in SLC and SLCd. It is found that this temperature is clearly lower for the softer symmetry energy that gives higher values in the low-density region where the LG phase transition occurs. This is understandable because at given temperatures it is easier to access to a larger isospin asymmetry in asymmetric matter with a smaller symmetry energy of the model. However, the temperature determined from a point of inflection is not the critical temperature for asymmetric matter. In deed, with the conserved isospin asymmetry of asymmetric matter the pressure and chemical potentials in the LG coexisting phase change throughout the transition [5], in contrast to the case of symmetric matter. The calculation of the critical temperature  $T_c$  in asymmetric matter is thus different, and we will calculate the  $T_c$  later on.

Now, we turn to the discussion on the LG phase transition in asymmetric nuclear matter according to the Gibbs conditions (10) and (11). For a fixed pressure, the two solutions of the LG phases to the Gibbs conditions form the edges of a rectangle in the proton and neutron chemical potential isobars as a function of isospin asymmetry  $\alpha$  and can be found by means of the geometrical construction method [5,9]. We thus

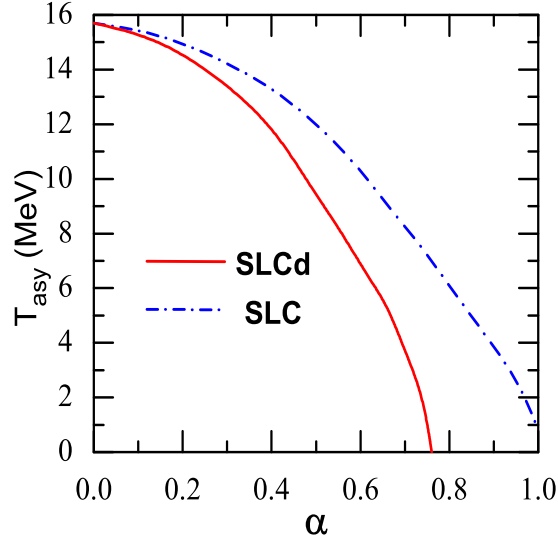


Fig. 2. (Color online) The temperature  $T_{asy}$  versus the asymmetry parameter  $\alpha$  in SLCd and SLC.

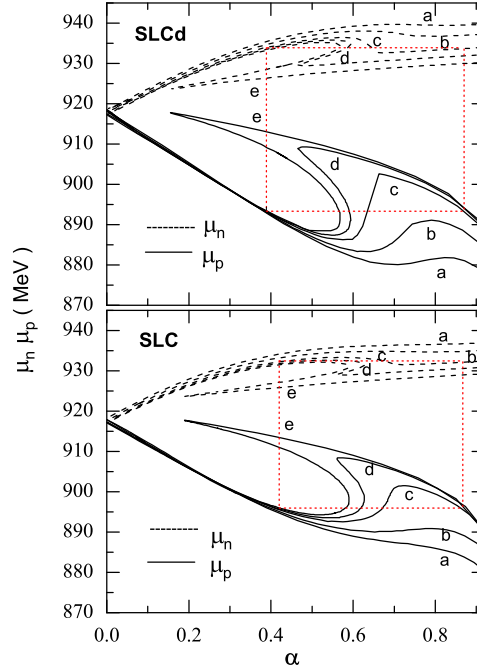


Fig. 3. (Color online) Chemical potential isobars as a function of  $\alpha$  at temperature  $T = 10$  MeV. The curves a, b, c, d, and e correspond to the pressures  $p = 0.235, 0.175, 0.12, 0.098,$  and  $0.08 \text{ MeV fm}^{-3}$  in SLCd and SLC, respectively. The rectangle, an example for the geometrical construction for  $p = 0.12 \text{ MeV fm}^{-3}$ , is used to determine the asymmetry parameters and chemical potentials in the LG coexistence phase.

need firstly to obtain the proton and neutron chemical potential isobars. The chemical potentials of the proton and neutron, together with the isospin asymmetry parameter, are numerically determined at given pressures and densities. Fig. 3 shows the  $\mu_n$  and  $\mu_p$  isobars as a function of  $\alpha$  at fixed temperature  $T = 10$  MeV for various pressures.

The solid and dashed curves are for protons and neutrons, respectively. We see that the curves for lower pressures are more complicated than those for higher pressures. Using the geometrical construction in the chemical potential isobars, we can then obtain two solutions at different isospin asymmetry parameters  $\alpha$  for two phases under the chemical and mechanical equilibria. As an example, we plot the rectangle for the case of  $T = 10\text{MeV}$  and  $p = 0.12\text{MeVfm}^{-3}$  in Fig. 3. The solution with the larger  $\alpha$  defines the gas phase with the lower density, while the solution with the smaller  $\alpha$  defines the liquid phase with the higher density.

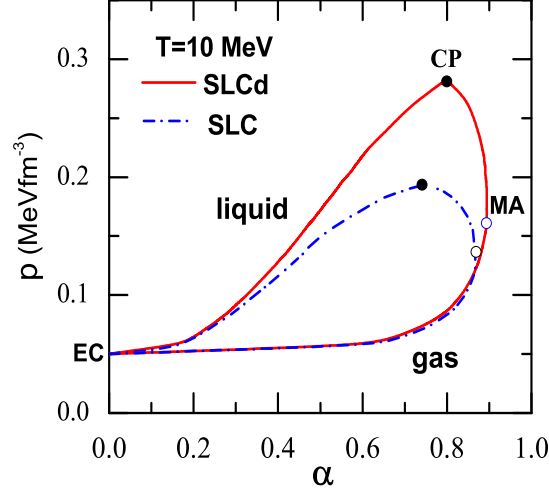


Fig. 4. (Color online) The section of the binodal surface at  $T = 10\text{ MeV}$  in SLCd and SLC. The CP, MA and EC stand for the critical point, the maximal isospin asymmetry and the point of equal concentration, respectively.

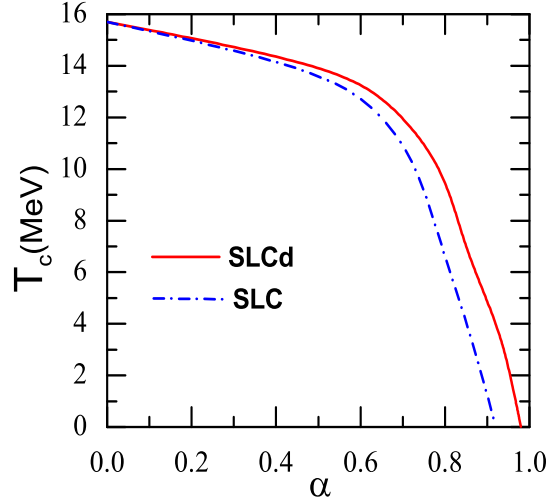


Fig. 5. (Color online) The critical temperature  $T_c$  versus the asymmetry parameter  $\alpha$  in SLCd and SLC.

The pair of the solutions of the Gibbs conditions found by the geometrical method forms the phase-separation boundary at a given pressure in hot asymmetric nuclear matter, while all pairs build up the binodal surface. In Fig. 4, we show the section of

the binodal surface at  $T=10$  MeV. The binodal surface is divided into two branches by the critical point (CP)  $(\alpha_c, p_c)$  and the point of the equal concentration (EC)  $(\alpha = 0)$ . One branch is the high-density (liquid) phase, and the other branch is the low-density (gas) phase. We see in Fig. 4 that a much higher CP and a much larger boundary of the phase coexistence appear in SLCd, compared with those in SLC. This indicates that the section of the binodal surface is very sensitive to the density dependence of the symmetry energy, because the unique difference between the SLCd and SLC is that the former possesses the much softer symmetry energy than that in the latter. Similar sensitivity was found in Refs. [15,16]. Also, we see that the softness of the symmetry energy in SLCd makes the maximal asymmetry (MA) a little larger, as compared with the MA in SLC.

As shown in the binodal curve in Fig. 4, the system can only be in a single phase for  $\alpha > \alpha_c$  at a given temperature. Correspondingly, at a fixed  $\alpha$  ( $\alpha = \alpha_c$ ) the given temperature plays a role of the critical temperature  $T_c$  beyond which the system totally cannot fall into the liquid phase at all pressures. In this way, one can obtain the critical temperatures at various  $\alpha$ . In Fig. 5, we depict  $T_c$  as a function of  $\alpha$  in SLC and SLCd. It is seen that the critical temperature separating a single phase from the coexisting liquid-gas phase decreases rapidly with increasing the isospin asymmetry parameter  $\alpha \geq 0.6$ . We find from Fig. 5 that  $T_c$  is higher for the model with the softer symmetry energy (SLCd) that gives higher value of the symmetry energy in the low-density region where the LG phase transition occurs. Our finding is in agreement with that in Ref. [16]. Interestingly, we find that the sensitivity of  $T_c$  to differences in the symmetry energy is exactly in contrast to that of  $T_{asy}$  as shown in Fig. 2. As seen in Fig. 5,  $T_c$  is not very typically sensitive to differences in the symmetry energy. In deed, the symmetry energy relies also on the temperature. In order to exhibit the dependence of the critical temperature on the symmetry energy, we draw in Fig. 6 the ratios of the critical temperature  $T_c$  to the symmetry energy, the slope and the curvature modulus as a function of the isospin asymmetry. The symmetry energy is here expanded at density  $\rho_h = 0.08 fm^{-3}$  as

$$E_{sym}(\rho_B, T) = E_{sym}(\rho_h, T) + \frac{L}{3}\chi_h + \frac{\kappa_{sym}}{18}\chi_h^2 + \dots, \quad (12)$$

where  $L$  and  $\kappa_{sym}$  are the slope and curvature of the symmetry energy at  $\rho_h = 0.08 fm^{-3}$ , and  $\chi_h = (\rho_B - \rho_h)/\rho_h$ . The reason for choosing  $\rho_h = 0.08 fm^{-3}$  is due to the facts that the critical density at the critical point is below but close to  $0.08 fm^{-3}$  and that this density may be regarded as an average density over the surface and volume of finite nuclei [29]. We see from Fig. 6 that the ratios of the  $T_c$  to the symmetry energy and its slope are just moderately different for the SLCd and SLC, while the distinction is surprisingly large for the curvature. This demonstrates that at the given symmetry energy and slope the  $T_c$  is moderately different for the SLCd and SLC, consistent with the result shown in Fig. 5. Though in the right panel of Fig. 6 the large departure can be observed for the  $T_c$  at given curvatures, the final role of the curvature is restrained by the factor  $\chi_h^2$  which is quite small in the present case. Moreover, we find that the



slope and curvature terms in Eq.(12) play an opposite role to that of the zero-order term in affecting the critical temperature. As a result, the critical temperature in hot asymmetric matter is just moderately model dependent, as shown in Fig. 5.

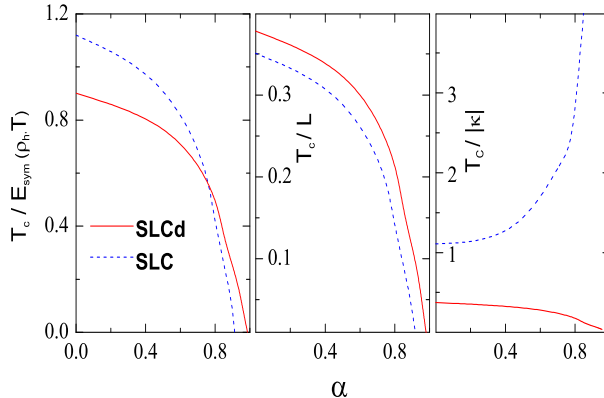


Fig. 6. (Color online) Ratios of the critical temperature  $T_c$  to the symmetry energy (left), the slope  $L$  (middle) and the curvature modulus  $|\kappa|$  (right) as a function of the isospin asymmetry. The slope and curvature of the symmetry energy are also calculated at density  $\rho_h$ .

At last, it is interesting to point out that the limiting pressure in the binodal surface does not appear in the present models. As pointed out in Refs. [9,13], the limiting pressure that is a cutoff of the pressure beyond which the pair of the solution does not exist in the geometrical construction is a result of the density dependence of the  $\rho$  meson-nucleon vertex. However, this seems to be rather model-dependent. In deed, the difference in values of the limiting pressure is large in models applied in Refs. [9,13]. In some nonlinear RMF models [16] where the density dependence of the  $\rho$  meson-nucleon interaction is actually induced by  $\rho$ -meson effective mass, the limiting pressure also does not appear.

## 4 SUMMARY

In summary, we have investigated the effects of the nuclear EOS with the density-dependent interactions on the liquid-gas phase transition in symmetric and asymmetric nuclear matter with the well-constrained RMF models SLCd and SLC that feature in-medium hadron properties according to the BR scaling and can provide satisfactory description for properties of finite nuclei and neutron stars. The critical temperature of the LG phase transition in symmetric matter is obtained to be 15.7 MeV for both models that have the same symmetric part of the nuclear EOS, in nice agreement with experimental data. With an analytic continuation from symmetric to asymmetric matter, we have obtained a temperature  $T_{asy}$  in hot asymmetric matter according to the monotonicity of the pressure and demonstrated that this temperature is lower for the softer symmetry energy. It is found in hot asymmetric matter that the boundary

of the phase-coexistence region is very sensitive to differences in the symmetry energy in SLC and SLCd, while the dependence on the EOS of symmetric matter is much weaker. A higher pressure and a larger area of the LG phase coexistence region appear with a softer symmetry energy. The critical temperature of hot asymmetric matter that separates the single-phase region from the two-phase region is found to be higher for the model with the softer symmetry energy, while the magnitude of the sensitivity is analyzed to be just moderate as compared with that for the boundary of the LG phase coexistence.

## Acknowledgement

We would like to thank Lie-Wen Chen and Chen Wu for useful discussions. The work was supported in part by the National Natural Science Foundation of China under Grant Nos. 10975033 and 11275048 and the China Jiangsu Provincial Natural Science Foundation under Grant No.BK2009261.

## References

- [1] D. Q. Lamb, J. M. Lattimer, C. J. Pethick, D. G. Ravenhall, *Phys. Rev. Lett.* **41**, 1623 (1978).
- [2] G. F. Bertsch, P. J. Siemens, *Phys. Lett. B* **126**, 9 (1983).
- [3] H. Jaqaman, A. Z. Mekjian, L. Zamick, *Phys. Rev. C* **29**, 2067 (1984).
- [4] H. Q. Song and R. K. Su, *Phys. Rev. C* **44**, 2505 (1991).
- [5] H. Müller and B. D. Serot, *Phys. Rev. C* **52**, 2072 (1995).
- [6] Y. G. Ma et al. *Phys. Lett. B* **390**, 41 (1997).
- [7] W. L. Qian, R. K. Su, and H. Q. Song, *J. Phys. G* **28**, 379 (2002).
- [8] M. Baldo and L. S. Ferreira, *Phys. Rev. C* **59**, 682(1999).
- [9] W. L. Qian, R. K. Su, and P. Wang, *Phys. Lett. B* **491**, 90 (2000).
- [10] J. B. Natowitz, K. Hagel, Y. Ma, M. Murray, L. Qin, R. Wada, and J. Wang, *Phys. Rev. Lett.* **89**,212701(2002).
- [11] Ph. Chomaz, M. Colonna, and J. Randrup, *Phys. Rep.* **389**, 263 (2004).
- [12] A. Rios, *Nucl. Phys. A* **845**, 58 (2010).
- [13] C. Wu and Z. Ren, *Phys. Rev. C* **83**, 044605 (2011).

- [14] R. Aguirre, Phys. Rev. C **85**, 014318 (2012).
- [15] J. Xu, L. W. Chen, B. A. Li, and H. R. Ma, Phys. Lett. B **650**, 348 (2007).
- [16] B. K. Sharma and S. Pal, Phys. Rev. C **81**, 064304 (2010).
- [17] B. A. Li, L. W. Chen, and C. M. Ko, Phys. Rep. **464**, 113 (2008).
- [18] B. A. Brown, Phys. Rev. Lett. **85**, 5296 (2000).
- [19] C. J. Horowitz and J. Piekarewicz, Phys. Rev. Lett. **86**, 5647 (2001).
- [20] W. Z. Jiang, B. A. Li, and L. W. Chen, Phys. Lett. B **653**, 184 (2007).
- [21] W. Z. Jiang, B. A. Li, and L. W. Chen, Phys. Rev. C **76**, 054314 (2007).
- [22] G. E. Brown and M. Rho, Phys. Rev. Lett. **66**, 2720 (1991).
- [23] G. E. Brown, J. W. Holt, C.-H. Lee, and M. Rho, Phys. Rep. **439**, 161 (2007).
- [24] X. M. Jin and D. B. Leinweber, Phys. Rev. C **52**, 3344 (1995).
- [25] D. Trnka, et. al., Phys. Rev. Lett. **94**, 192303 (2005).
- [26] M. Naruki, et. al., Phys. Rev. Lett. **96**, 092301 (2006).
- [27] B. Schenke and C. Greiner, Phys. Rev. Lett. **98**, 022301 (2007).
- [28] J. W. Holt, G. E. Brown, T. T. S. Kuo, J. D. Holt, and R. Machleidt, Phys. Rev. Lett. **100**, 062501 (2008).
- [29] L. W. Chen, Phys. Rev. C **83**, 044308 (2011).